IOPscience iopscience.iop.org

Home Search Collections Journals About Contact us My IOPscience

The modulation of the de Haas–van Alphen effect in graphene by electric field

This article has been downloaded from IOPscience. Please scroll down to see the full text article.

2010 J. Phys.: Condens. Matter 22 115302

(http://iopscience.iop.org/0953-8984/22/11/115302)

View the table of contents for this issue, or go to the journal homepage for more

Download details:
IP Address: 129.252.86.83
The article was downloaded on 30/05/2010 at 07:34

Please note that terms and conditions apply.

J. Phys.: Condens. Matter **22** (2010) 115302 (8pp) doi:10.1088/0953-8984/22/11/115302

The modulation of the de Haas–van Alphen effect in graphene by electric field

Shengli Zhang[1,2], **Ning Ma**[1] **and Erhu Zhang**[1]

[1] Department of Applied Physics, Xi'an Jiaotong University, Xi'an 710049, People's Republic of China
[2] MOE Key Laboratory for Nonequilibrium Synthesis and Modulation of Condensed Matter, Xi'an Jiaotong University, Xi'an 710049, People's Republic of China

Received 12 September 2009, in final form 4 January 2010
Published 23 February 2010
Online at stacks.iop.org/JPhysCM/22/115302

Abstract

This paper explores the de Haas–van Alphen effect (dHvA) of graphene in the presence of an in-plane uniform electric field. Three major findings are yielded. First of all, the electric field is found to modulate the de Haas–van Alphen magnetization and magnetic susceptibility through the dimensionless parameter ($\beta = \frac{E}{v_F B}$). As the parameter β increases, the values of magnetization and magnetic susceptibility increase to positive infinity or decrease to negative infinity at the exotic point $\beta_c = 1$. Furthermore, the dHvA oscillation amplitude rises abruptly to infinity for zero temperature at $\beta_c = 1$, but eventually collapses at a finite temperature, thereby leading to the de Haas–van Alphen effect vanishing. In addition, the magnetic susceptibility depends on the electric and magnetic fields, suggesting that graphene should be a non-linear magnetic medium in the presence of an external field. These results, which are different from those obtained in the standard non-relativistic 2D electron gas, are attributed to the anomalous Landau level spectrum of graphene.

(Some figures in this article are in colour only in the electronic version)

1. Introduction

Owing to the progress in experimental methods, graphene (or a graphite monolayer) is now attracting increasing interest in the field of the physics of electronic systems with reduced dimensionality [1–4]. It is promising for application in nanoelectronics because of the exotic chiral features [5–9] in its electronic structure. In particular, such two-dimensional (2D) or quasi-two-dimensional systems have led to some of the most startling discoveries in condensed matter physics in recent years. Moreover, these anomalous phenomena are found to be tied to the remarkable 'relativistic-like' spectrum of electrons and holes in graphene, which makes graphene important and interesting in physics. One of those that have been experimentally testified is the abnormality of the 2D quantum Hall effect [10, 11].

Another important physics effect is the de Haas–van Alphen (dHvA) oscillation of graphene. It has been predicted in [12], which proposes that the magnetization oscillates periodically in a sawtooth pattern as a function of $1/B$, in agreement with the Peierls prediction [13]. A question of great interest arising here is what will happen if an additional electric field is applied in graphene. Indeed, the electric and magnetic field effects on its magnetization and magnetic susceptibility are of vital significance to our understanding of the Dirac fermion behavior. However, little theoretical or experimental research has been done on this issue yet.

Motivated by the concerns mentioned above, the present study is to investigate the 2D dHvA effect of graphene in the presence of an electric field. The paper is organized as follows. In section 2, a brief introduction is given to the 2D model for graphene. The energy eigenvalues and eigenstates, as well as the density of states (DOS) and the dHvA oscillation period $\Delta(1/B)$ are obtained analytically. Section 3 describes some details of the magnetization and magnetic susceptibility study. Analytical expressions are derived for the magnetization and magnetic susceptibility. More specifically, the one regarding the condition of $T = 0$ K is reported in section 3.1 while the one pertaining to the condition of nonzero temperature is covered in section 3.2. The section winds up with a discussion of the modulation of dHvA in graphene by an electric field. In section 4, the conclusions are presented.

2. Energy eigenvalues and eigenstates

In order to investigate the modulation of dHvA, we begin with the study of the energy eigenvalues and eigenstates belonging

 © 2010 IOP Publishing Ltd Printed in the UK

to the carriers in graphene. The charge carriers in graphene mimic relativistic particles with zero rest mass and have the effective 'speed of light' $c^* = \upsilon_F \approx 1.0 \times 10^6$ m s^{-1}, which is essentially governed by the Dirac equation [10, 11]. So we start by considering the Dirac equation for such a 2D gas of Dirac fermions in crossed electric $[\vec{E} = (-E, 0, 0), U = Eex]$ and magnetic $[\vec{B} = (0, 0, B), \vec{A} = (0, Bx, 0)]$ fields, where E is the electric field strength and B the magnetic induction intensity. The single particle Hamiltonian is then given by

$$\hat{H} = \upsilon_F \hat{\boldsymbol{\alpha}} \cdot \boldsymbol{\Pi} + \hat{\mathbf{I}} eEx \tag{1}$$

in which $\hat{\boldsymbol{\alpha}}$ is the Pauli matrix, Π is the canonical momentum and $\hat{\boldsymbol{I}}$ is the 2×2 unit matrix. Following Landau and Lifshitz [14], the first-order equation of the eigenvalue problem of $\hat{H}$ becomes the second-order equation

$$[(\varepsilon - eEx)^2 - (\upsilon_F \vec{p} - e\vec{A})^2 + e\hbar B \upsilon_F^2 \hat{\boldsymbol{\alpha}}_z + \mathrm{i}e\hbar E \upsilon_F \hat{\boldsymbol{\alpha}}_x]\Psi = 0, \tag{2}$$

where ε is the eigenvalue of $\hat{H}$ and the other notation is standard. From equation (2), we obtain the energy spectra and eigenfunctions of the problem,

$$\varepsilon_{n,k_y} = \mathrm{sgn}(n)\sqrt{2|n|\hbar e B}\upsilon_F(1-\beta^2)^{3/4} + \hbar \upsilon_F \beta k_y, \tag{3}$$

$$\Psi_{n,k_y}(x, y) \propto \exp(\mathrm{i}k_y y)\exp[-(\beta/2)\alpha_y] \times \begin{pmatrix} \mathrm{sgn}(n)i^{|n|-1}\phi_{|n|-1}(\xi) \\ \mathrm{i}^{|n|}\phi_n(\xi) \end{pmatrix}, \tag{4}$$

with

$$\xi \equiv \frac{(1-\beta^2)^{1/4}}{l_c}\left(x + l_c^2 k_y - \mathrm{sgn}(n)\frac{\sqrt{2|n|}l_c\beta}{(1-\beta^2)^{1/4}}\right). \tag{5}$$

In equation (3), e and $\hbar = h/2\pi$ are the electron charge and Planck's constant divided by 2π, respectively. The integer n represents the Landau level index, $k_y = 2\pi l/L_y (l = 0, \pm1, \pm2, \ldots,)$ is the quantum number corresponding to the translation symmetry along the y axis, L_y stands for the size of the graphene in the y direction. The electric field dependent dimensionless parameter β is defined by $\beta = E/(\upsilon_F B)$ and obeys $|\beta| < 1$, where υ_F is the Fermi velocity. In equation (4), $\phi_n(\xi)$ are the harmonic oscillator eigenfunctions. From equation (5) we observe that the centers of the x-dependent orbits are located at

$$x_0 = l_c^2 k_y - \mathrm{sgn}(n)\frac{\sqrt{2|n|}l_c\beta}{(1-\beta^2)^{1/4}}, \tag{6}$$

where $l_c = \sqrt{\hbar/eB}$ is the magnetic length. The eigenvalues of $\hat{H}$ show that the exact energies are given by the sum of the quantized harmonic oscillator energies and the potential energy of a charged particle located at coordinate x_0 in a potential field $U(x)$. They agree with those in [15], the authors of which solved the problem by transforming the original system into a case with a null electric field, in terms of a Lorentz boost transformation.

We then count the Landau states Ψ_{n,k_y} in the presence of the potential $U(x)$, following the same argument employed in the absence of a crossed electric field. Since $k_y = 2\pi l/L_y$, the separation between adjacent allowed k_y values is given by $\delta k_y = 2\pi/L_y$. From equation (6) we may relate the possible range Δk_y of k_y to the physically accessible range Δx_0 of x_0:

$$\Delta x_0 = l_c^2 \Delta k_y. \tag{7}$$

Since $\Delta x_0 = L_x$, in order for the Landau states to be centered within the strip $0 \leqslant x_0 \leqslant L_x$ we must allow the range of k_y values given by $\Delta k_y = \Delta x_0/l_c^2$. The number of Landau states $\Psi_{n,k_y}(x, y)$ per unit area for each quantum number n is:

$$D_n = \frac{g_s \Delta k_y}{L_x L_y \delta k_y} = \frac{2eB}{\hbar\pi}, \tag{8}$$

which is independent of n, and the degeneracy yields $g_s = 4$, accounting for the spin degeneracy and sublattice degeneracy in graphene.

We consider a system of N electrons within an area S moving in the potential $U(x)$ and the magnetic field B. Let the system remain at 0 K and accordingly the free energy reduces to the total energy. The full occupation of Landau levels obeys $D_n S = N/(n_F + 1)$, with Fermi quantum number n_F. The total energy $E = \sum_{n,k_y} \varepsilon_{n,k_y}(B)$ will give a discontinuous derivative $M = -\partial E/\partial B$ at the field values B_n, where M is the magnetization. From $D_n S = N/(n_F + 1)$ these discontinuities in the magnetization occur at reciprocal fields $1/B_n$, so that the period of magnetization oscillation is given by:

$$\Delta\left(\frac{1}{B}\right) = \frac{1}{B_{n+1}} - \frac{1}{B_n} = \frac{2e}{\pi\hbar N_0}, \tag{9}$$

where B_{n+1} and B_n are the magnetic induction intensity corresponding to two neighboring levels which cross the Fermi level in succession, and $N_0 = N/S$ is the sheet concentration. Equation (9) means that the discontinuous zero temperature oscillations are periodic in $1/B$. It is just compatible with the results regarding the null electric field obtained by Sharapov *et al* [12].

3. Magnetization and magnetic susceptibility

3.1. Zero temperature

Now we move on to investigate the magnetization of electrons in graphene in the presence of crossed uniform electric and magnetic fields at $T = 0$ K. For simplicity, we ignore spin–orbit coupling of electrons in the present work. The magnetization reads [16, 17]

$$M = -(\partial E/\partial B)_N, \tag{10}$$

where E is the total energy and N denotes the total number of electrons in graphene. To have the units in tesla, we symbolize $B = \mu_{p0}H$, μ_{p0} as being the magnetic permeability of free space, H stands for the magnetic field intensity.

The total energy is given by:

$$E = \sum_{n,k_y} \varepsilon_{n,k_y} = \sum_{n=0}^{[\mu_0^2/2e\hbar\upsilon_F^2 B]} D_n(\varepsilon_n - \mu) + \mu N_0 + \sum_{l=-l_F}^{l_y} \frac{2\pi}{L_y}\hbar\upsilon_F\beta l, \qquad (-l_F \leqslant l_y \leqslant l_F) \tag{11}$$

in which the last term is the additional energy induced by the electric field corresponding to the n_Fth level partly occupied by electrons and which we refer to as E_{add}. Here ε_n is defined as $\varepsilon_n = \sqrt{2n\hbar eB}\upsilon_F(1-\beta^2)^{3/4}$. The chemical potential $\mu = \mu_0(1-\beta^2)^{3/4}$ is derived analytically, where μ_0 refers to the zero temperature chemical potential (equal to the Fermi energy) in the absence of electric and magnetic fields, as expressed by $\mu_0 = \hbar\upsilon_F\sqrt{N_0\pi}$. Using the formula for the generalized zeta function [18], $\zeta(z,\upsilon+k) = \zeta(z,\upsilon) - \sum_{m=0}^{k-1}(m+\upsilon)^{-z}$ and $\zeta(-1/2,0) \equiv \zeta(-1/2) \equiv -(1/4\pi)\zeta(3/2)$, one can write the first and the second terms in equation (11) as the summation of the regular term,

$$E_{reg} = -\frac{\zeta(3/2)\upsilon_F}{\pi^2\sqrt{2\hbar}}(eB)^{3/2}(1-\beta^2)^{3/4} + \frac{2\mu_0^3}{3\pi(\hbar\upsilon_F)^2}(1-\beta^2)^{3/4}, \tag{12}$$

and the oscillating term

$$\begin{aligned} E_{osc} = &-\frac{2\sqrt{2\hbar}\upsilon_F}{\pi\hbar}(eB)^{3/2}(1-\beta^2)^{3/4}\zeta \\ &\times\left(-\frac{1}{2}, 1+\left[\frac{\mu_0^2}{2e\hbar\upsilon_F^2B}\right]\right) - (1-\beta^2)^{3/4} \\ &\times\left[\frac{2\mu_0^3}{3\pi(\hbar\upsilon_F)^2} - \frac{2\mu_0 eB}{\pi\hbar}\left(\mathrm{mod}\left[\frac{\mu_0^2}{2e\hbar\upsilon_F^2B}\right] - \frac{1}{2}\right)\right]. \end{aligned} \tag{13}$$

In this expression, $[\mu_0^2/2e\hbar\upsilon_F^2B]$ stands for the integer part of $\mu_0^2/2e\hbar\upsilon_F^2B$ and the mod$[\mu_0^2/2e\hbar\upsilon_F^2B]$ is the fractional part of $\mu_0^2/2e\hbar\upsilon_F^2B$.

Making use of the Γ function $\Gamma(n+\alpha) = \int_0^\infty \mathrm{d}s\, s^{n+\alpha-1}\mathrm{e}^{-s}$ and Bernoulli polynomials $B_n(y)$, $\sum_{n=0}^\infty \frac{x^n}{n!}B_n(y) = \frac{x\mathrm{e}^{xy}}{\mathrm{e}^x-1}$, $(|x|<2\pi)$, we obtain

$$\begin{aligned} &\sum_{n=2}^\infty \frac{\Gamma(n+\alpha)B_n(y)}{n!}x^n \\ &= \int_0^\infty \mathrm{d}s\, s^{\alpha-1}\mathrm{e}^{-s}\left[\frac{sx\mathrm{e}^{sxy}}{\mathrm{e}^{sx}-1} - 1 - sxB_1(y)\right], \end{aligned} \tag{14}$$

where the explicit expressions for the Bernoulli polynomials B_0, B_1, B_2 are

$$\begin{aligned} B_0(y) = 1, \qquad B_1(y) = y - 1/2, \\ B_2(y) = y^2 - y - 1/6. \end{aligned} \tag{15}$$

The Bernoulli polynomials depend on mod$[y]$ in the following equations, i.e. $B_n(\mathrm{mod}[y])$. For brevity, we write this as $B_n(y)$.

Using the formula [17]

$$\int_0^\infty \frac{x^{v-1}\mathrm{e}^{-\mu x}\mathrm{d}x}{1-\mathrm{e}^{-\beta x}} = \frac{1}{\beta^v}\Gamma(v)\zeta\left(v, \frac{\mu}{\beta}\right), \quad (\mathrm{Re}\,\mu > 0, \mathrm{Re}\,v > 0)$$

we have

$$\begin{aligned} E_{osc} = &\frac{2(eB\upsilon_F)^2}{\pi^{3/2}\mu_0}(1-\beta^2)^{3/4} \\ &\times\sum_{n=0}^\infty \frac{\Gamma(n+1/2)B_{n+2}(w/2)}{(n+2)!}\left(\frac{2e\hbar\upsilon_F^2B}{\mu_0^2}\right)^n, \end{aligned} \tag{16}$$

in which $w = \mu_0^2/(e\hbar\upsilon_F^2B)$. Regarding small fields, $eB\hbar\upsilon_F^2 \ll \mu_0^2$, we can apply the following asymptotic expansions for $J_1 = \int_0^\infty \mathrm{d}t\, \mathrm{e}^{-tp}/[\sqrt{\pi t}(t^2+1)]$:

$$J_1(p) = \frac{1}{\sqrt{\pi}}\sum_{n=0}^\infty \frac{(-1)^n\Gamma(n+1/2)}{p^{n+1/2}} \tag{17}$$

and the Bernoulli polynomials B_n periodically continue beyond the interval [0, 1]:

$$\begin{aligned} B_n = &-\frac{2n!}{(2\pi)^n}\sum_{k=1}^\infty \frac{1}{k^n}\cos\left(2\pi kx - \frac{n\pi}{2}\right), \\ &n>1, \quad 0\leqslant x\leqslant 1; \quad n=1, 0<x<1. \end{aligned} \tag{18}$$

It is easy to get the following form:

$$E_{osc} = \frac{(eB)^{3/2}\upsilon_F}{\sqrt{\hbar}\pi}(1-\beta^2)^{3/4}\sum_{k=1}^\infty \frac{1}{(\pi k)^{3/2}}J_1(\pi kw)\cos(\pi kw). \tag{19}$$

For $\sqrt{eB\hbar\upsilon_F^2} \ll \mu_0$, keeping the leading term in the asymptotic expansions for $J_1(p)$, we finally obtain from equation (19)

$$E_{osc} \cong \frac{(eB\upsilon_F)^2}{\pi\mu_0}(1-\beta^2)^{3/4}\sum_{k=1}^\infty \frac{\cos(\pi kw)}{(\pi k)^2}. \tag{20}$$

Hence the total energy E can be expressed as a sum of regular, oscillating and additional energy terms,

$$E = E_{reg} + E_{osc} + E_{add}. \tag{21}$$

According to the results reported above, we get the corresponding de Haas–van Alphen magnetization,

$$M_{reg} = \frac{3e\sqrt{eB\hbar}\varsigma(3/2)\upsilon_F}{2\sqrt{2}\pi^2\hbar(1-\beta^2)^{1/4}} - \frac{\mu_0^3\beta^2}{\pi(\hbar\upsilon_F)^2B(1-\beta^2)^{1/4}}, \tag{22}$$

$$M_{add} = \frac{\pi\hbar\upsilon_F\beta}{BL_y}A_{M_0}, \tag{23}$$

where

$$A_{M_0} = \left[\frac{\mu_0^4}{\pi^2(\hbar\upsilon_F)^4} - \left[\frac{\mu_0^2}{2e\hbar\upsilon_F^2B}\right]\left(\left[\frac{\mu_0^2}{2e\hbar\upsilon_F^2B}\right]+1\right)\left(\frac{2eB}{\hbar\pi}\right)^2\right]. \tag{24}$$

This expression involves a dependence on the integer part $[\mu_0^2/2e\hbar\upsilon_F^2B]$ and

$$\begin{aligned} M_{osc} = &A_{M1}\sum_{k=1}^\infty \frac{(-1)^k}{\pi k}\sin\left(\frac{\pi k\mu_0^2}{e\hbar\upsilon_F^2B}\right) \\ &+ A_{M2}\sum_{k=1}^\infty \frac{(-1)^k}{(\pi k)^2}\cos\left(\frac{\pi k\mu_0^2}{e\hbar\upsilon_F^2B}\right), \end{aligned} \tag{25}$$

where $A_{M1} = -\frac{e\mu_0(1-\beta^2)^{3/4}}{\pi\hbar}$ and $A_{M2} = -\frac{(e\upsilon_F)^2B(4-\beta^2)}{2\pi\mu_0(1-\beta^2)^{1/4}}$.

Figure 1 shows that the dHvA oscillation on the magnetization M is modulated by the electric field in graphene. As shown in figure 1(a), the magnetization M oscillates periodically in $1/B$ with a period of $\Delta(1/B) = 2e\hbar\upsilon_F^2/\mu_0^2$. The three oscillation curves correspond to applied electric field strengths $E_1 = 5\ \mathrm{V\,m^{-1}}$, $E_2 = 10\ \mathrm{V\,m^{-1}}$ and $E_3 = 15\ \mathrm{V\,m^{-1}}$, respectively. From these curves, one can see that the oscillation amplitude (OA) of magnetization is proportional

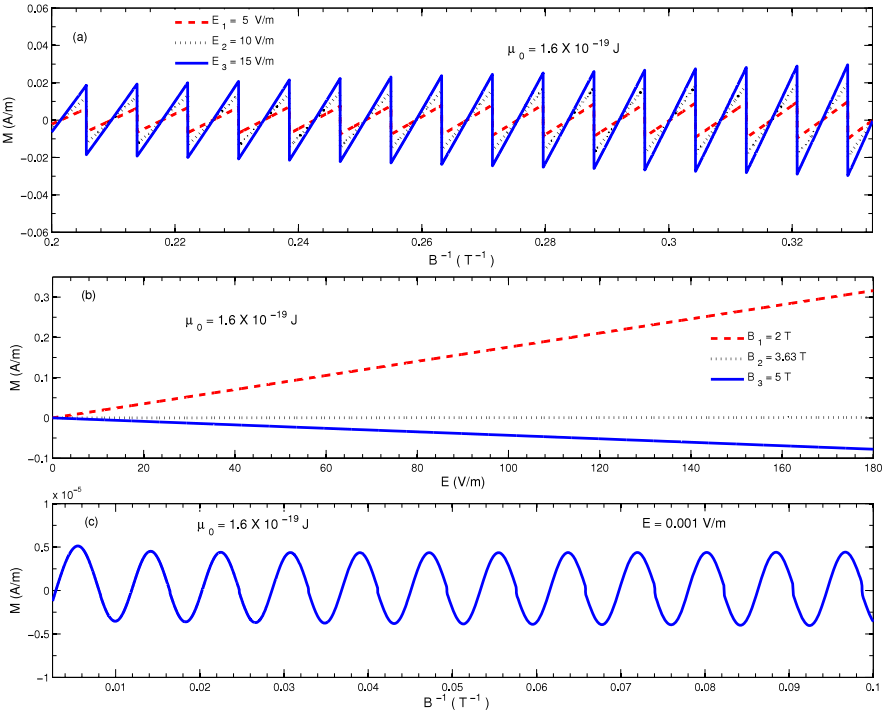

Figure 1. (a) Magnetization M is plotted as a function of reciprocal magnetic field $1/B$ for a given chemical potential $\mu_0 = 1.6 \times 10^{-19}$ J and $T = 0$ K. The three oscillation curves correspond to $E_1 = 5$ V m^{-1}, $E_2 = 10$ V m^{-1} and $E_3 = 15$ V m^{-1}, respectively. (b) M plotted versus electric field E for $\mu_0 = 1.6 \times 10^{-19}$ J and $T = 0$ K. The three curves correspond to $B_1 = 2$ T, $B_2 = 3.63$ T and $B_3 = 5$ T, respectively. (c) The magnetization, M, as a function of $1/B$ at $E = 0.001$ V m^{-1}, $\mu_0 = 1.6 \times 10^{-19}$ J and $T = 0$ K.

to the electric field E. Also, the OA grows significantly with increasing $1/B$, but remains unchanged for the null electric field in [12]. Thus, the electric field effect on the OA of magnetization is demonstrated. However unexpected it may be, according to equation (25) the OA increases abruptly to infinity at $\beta_c = 1$, thereby leading to the vanishing of dHvA oscillation. It is interesting that the abnormal phenomena will die out if the electric field vanishes. Thus, it can be also attributed to the electric field effect. We hope that the new findings will be verified when magnetization experiments under an in-plane electric field are carried out in graphene. The predicted effect will hopefully also help the interpretation of magnetization in experiment.

In contrast, we find that these peculiar features are absent in standard quantum 2D electron gas systems [19–21]. Hence, a possible reason for the effect might be that it is determined by the 'relativistic' character of the carriers in graphene, unlike the usual sample, which can be traced to the exotic structure in graphene.

Figure 1(b) demonstrates that the magnetization M is a function of the electric field E. The three curves correspond to $B_1 = 2$ T, $B_2 = 3.63$ T and $B_3 = 5$ T, respectively. They show that the magnetization varies approximately linearly with increasing E within the given values of parameters. For $B_1 = 2$ T, the magnetization increases with increasing E. But for $B_3 = 5$ T, as E increases the magnetization decreases. In particular, there is a special behavior of the magnetization at some magnetic fields (e.g. $B_2 = 3.63$ T). In this case, the magnetization satisfies $M \simeq 0$, accounting for the disappearance of magnetization in graphene. Note that the magnetization become infinite when the variation of E obeys $\beta_c = 1$ according to equations (22) and (25). For example, the dashed line ($B_1 = 2$ T) rises abruptly to infinity at $E = 2 \times 10^6$ V m^{-1}, strikingly different from the non-relativistic results.

In figure 1(c), we present the dHvA effect for a wide range of magnetic fields, starting from 10 to 400 T, in order to examine what will happen if the magnetic field tends to infinity. As a result, we observe that on this scale, the electric field effect could be negligible, corresponding to the case $\beta \to 0$. In other words, for the case of $\beta \to 0$, the magnetization M reduces to the result for the null electric field.

The same discussion above fits for the magnetic susceptibility χ. We can obtain the expression for the dHvA magnetic susceptibility in terms of $\chi = \partial M/\partial H$,

$$\chi_{\rm reg} = \frac{3e\mu_{\rm p0}\sqrt{e\hbar}\zeta(3/2)\upsilon_{\rm F}}{4\sqrt{2B}\pi^2\hbar(1-\beta^2)^{5/4}}(1-2\beta^2) + \frac{\mu_0^3\beta^2\mu_{\rm p0}(6-5\beta^2)}{2\pi(\hbar\upsilon_{\rm F}B)^2(1-\beta^2)^{5/4}}, \tag{26}$$

$$\chi_{\rm add} = -\frac{2\mu_{\rm p0}\beta\mu_0^4}{L_y B^2(\hbar\upsilon_{\rm F})^3}, \tag{27}$$

and

$$\chi_{\rm osc} = (A_{\chi 1} + A_{\chi 2})\sum_{k=1}^{\infty}(-1)^k \cos\left[\frac{\pi k\mu_0^2}{e\hbar\upsilon_{\rm F}^2 B}\right] + (A_{\chi 3} + A_{\chi 4})\sum_{k=1}^{\infty}\frac{(-1)^k}{\pi k}\sin\left[\frac{\pi k\mu_0^2}{e\hbar\upsilon_{\rm F}^2 B}\right], \tag{28}$$

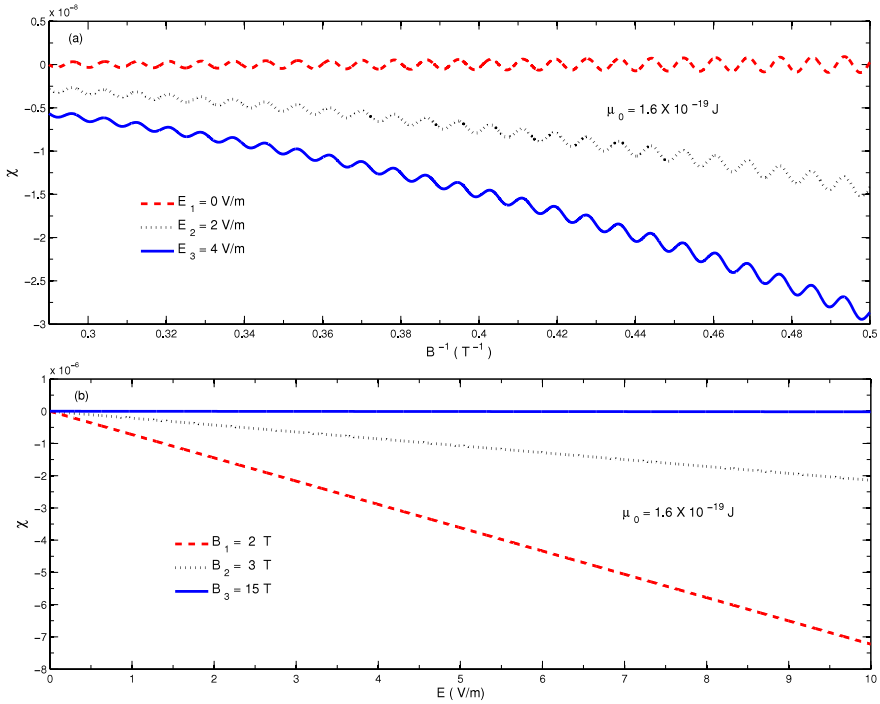

Figure 2. (a) Magnetic susceptibility χ depends on reciprocal field $1/B$ for a given chemical potential $\mu_0 = 1.6 \times 10^{-19}$ J and $T = 0$ K. The three oscillation curves of magnetic susceptibility correspond to $E_1 = 0$ V m^{-1}, $E_2 = 2$ V m^{-1} and $E_3 = 4$ V m^{-1}, respectively. (b) χ as a function of electric field E for $\mu_0 = 1.6 \times 10^{-19}$ J and $T = 0$ K. The three curves correspond to $B_1 = 2$ T, $B_2 = 3$ T and $B_3 = 15$ T, respectively.

where

$$A_{\chi 1} = \frac{\mu_{\rm p0}\mu_0^3(1-\beta^2)^{3/4}}{\pi(\hbar\upsilon_{\rm F}B)^2},$$
$$A_{\chi 2} = -\frac{(e\upsilon_{\rm F})^2\mu_{\rm p0}(8-10\beta^2-\beta^4)}{4\pi\mu_0(\pi k)^2(1-\beta^2)^{5/4}},$$
$$A_{\chi 3} = -\frac{\mu_{\rm p0}e\mu_0(4-\beta^2)}{2\pi\hbar B(1-\beta^2)^{1/4}}, \qquad (29)$$
$$A_{\chi 4} = -\frac{3\mu_{\rm p0}e\mu_0\beta^2}{2\pi\hbar B(1-\beta^2)^{1/4}}.$$

We can see that the magnetic susceptibility is related to both the electric and magnetic fields. It follows that, unlike the usual samples, graphene may be a non-linear magnetic medium.

Figure 2(a) shows that the magnetic susceptibility χ oscillates periodically as a function of $1/B$, and the period follows equation (9). The three oscillation curves correspond to $E_1 = 0$ V m^{-1}, $E_2 = 2$ V m^{-1} and $E_3 = 4$ V m^{-1}, respectively. For the case (E_1), the reader may observe that the magnetic susceptibility χ swings between negative and positive values, thus the curve shows a totally orbital diamagnetic to paramagnetic transition. As for the finite electric fields, one can see that the magnetic susceptibility decreases in company with the periodic oscillation, while $1/B$ rises and the OA augments as $1/B$ increases. Furthermore, from equation (28) it can be seen that the OA increases to infinity at $\beta_{\rm c} = 1$, leading to the vanishing of the dHvA effect on magnetic susceptibility. In general, the magnetic susceptibility χ is a constant in a usual electron gas, but in graphene it exhibits a dependence on the external field.

Figure 2(b) depicts the magnetic susceptibility χ with respect to the electric field E. The three curves correspond to $B_1 = 2$ T, $B_2 = 3$ T and $B_3 = 15$ T, respectively. As is shown by the three curves, the magnetic susceptibility varies approximately linearly with increasing E. For $B = 2$, or 3 T, the magnetic susceptibility decreases as E increases and yields $\chi < 0$, indicating the existence of Landau diamagnetism in graphene, the origin of which can be traced to the quantized Landau level. In the case of $B = 15$ T or larger, the magnetic susceptibility $\chi \simeq 0$ despite the increase of E, suggesting the disappearance of the diamagnetism in graphene. That is, there is no increase in the magnetic susceptibility with increasing E. Moreover, the dashed line ($B_1 = 2$ T) decreases to negative infinity at the exotic point $E = 2 \times 10^6$ V m^{-1} (i.e. $\beta_{\rm c} = 1$), as illustrated by equations (26) and (28).

3.2. Finite temperature

We now consider the temperature effect on the oscillations of magnetization and magnetic susceptibility. As documented in [12], the thermodynamic potential of electrons in graphene can be expressed as

$$\Omega(T,\mu) = \int_{-\infty}^{\infty} {\rm d}\omega\, P_T(\omega-\mu)E(\omega), \qquad (30)$$

with the energy variables ω and μ. Also $P_T(z)$ is the distribution function as

$$P_T(z) = -\frac{\partial n_{\rm F}(z)}{\partial z} = \frac{1}{4k_{\rm B}T\cosh^2\frac{z}{2k_{\rm B}T}}. \qquad (31)$$

Using equation (30), the thermodynamic potential Ω can be divided as follows:

$$\Omega(T,\mu) = \Omega_{\rm reg} + \Omega_{\rm add} + \Omega_{\rm osc}. \tag{32}$$

At low temperatures, neglecting $0(k_{\rm B}T)$, we can obtain

$$\Omega_{\rm reg} = -\frac{\zeta(3/2)\upsilon_{\rm F}}{\pi^2\sqrt{2\hbar}}(eB)^{3/2}(1-\beta^2)^{3/4} + \frac{2\mu_0^3}{3\pi(\hbar\upsilon_{\rm F})^2}(1-\beta^2)^{3/4}, \tag{33}$$

$$\Omega_{\rm add} = \frac{\pi}{L_y}\hbar\upsilon_{\rm F}\beta A_{\Omega_T} R_T(k,\mu), \tag{34}$$

where

$$A_{\Omega_T} = \frac{\mu_0^4}{\pi^2(\hbar\upsilon_{\rm F})^4} - \frac{2eB\mu_0^2}{\hbar(\pi\hbar\upsilon_{\rm F})^2}\left(2\left[\frac{\mu_0^2}{2e\hbar\upsilon_{\rm F}^2 B}\right]+1\right) + \left[\frac{\mu_0^2}{2e\hbar\upsilon_{\rm F}^2 B}\right]\left(\left[\frac{\mu_0^2}{2e\hbar\upsilon_{\rm F}^2 B}\right]+1\right)\left(\frac{2eB}{\hbar\pi}\right)^2. \tag{35}$$

This expression involves a dependence on the integer part $[\mu_0^2/2e\hbar\upsilon_{\rm F}^2 B]$. Here we introduced the temperature reduction factor

$$R_T(k,\mu) = \frac{2\pi^2 k\mu_0 k_{\rm B}T/(e\hbar\upsilon_{\rm F}^2 B^*)}{\sinh\frac{2\pi^2 k\mu_0 k_{\rm B}T}{e\hbar\upsilon_{\rm F}^2 B^*}}, \tag{36}$$

in which $B^* = B(1-\beta^2)^{3/4}$. Equation (36) means that the temperature reduction factor R_T depends not only on the temperature, but also on the electric and magnetic fields. We return now to the oscillating part of thermodynamic potential. Substituting equation (19) into equation (30), it is convenient to get the expression of $\Omega_{\rm osc}$ as

$$\Omega_{\rm osc}(T,\mu) = \frac{(eB)^{3/2}\upsilon_{\rm F}}{\sqrt{\hbar}\pi^{3/2}}(1-\beta^2)^{3/4}\sum_{k=1}^{\infty}\frac{1}{(\pi k)^{3/2}} \times {\rm Im}\left[{\rm e}^{-{\rm i}\pi/4}\int_0^\infty \frac{{\rm d}t\,{\rm e}^{-{\rm i}(\pi k w)t}}{\sqrt{t}(t+1)}\int_{-\infty}^{\infty}\frac{{\rm d}\epsilon}{4k_{\rm B}T\cosh^2\frac{(\epsilon-\mu)}{2k_{\rm B}T}} \times \exp\left(\frac{-{\rm i}\pi k\epsilon^2(t+1)}{e\hbar\upsilon_{\rm F}^2 B(1-\beta^2)^{3/2}}\right)\right], \tag{37}$$

in which we used that the function $J_1(p,r)$ and $J_2(p,r)$ which can be represented as the negative Im and Re parts of the same function

$$\sqrt{\pi}J_1(p,r) = -{\rm Im}\int_0^\infty \frac{{\rm d}t\,{\rm e}^{-pt-r/t}}{\sqrt{t}(t+i)}, \qquad \sqrt{\pi}J_2(p,r) = -{\rm Re}\int_0^\infty \frac{{\rm d}t\,{\rm e}^{-pt-r/t}}{\sqrt{t}(t+i)}, \tag{38}$$

and rotated the integration contour to the imaginary axis. Finally we get

$$\Omega_{\rm osc}(T,\mu) = \frac{(eB\upsilon_{\rm F})^2}{\pi\mu_0}(1-\beta^2)^{3/4}\sum_{k=1}^{\infty}\frac{\cos(\pi k w)}{(\pi k)^2}R_T(k,\mu), \tag{39}$$

with $w = \mu_0^2/(e\hbar\upsilon_{\rm F}^2 B)$. Clearly, since $R_T(k,\mu)\to 1$ for $T\to 0$, equation (39) reduces to the oscillating energy for zero temperature. When the temperature $T\neq 0$, the magnetization can be obtained as follows:

$$M_{\rm reg}^{\rm T} = \frac{3e\sqrt{eB\hbar}\zeta(3/2)\upsilon_{\rm F}}{2\sqrt{2}\pi^2\hbar(1-\beta^2)^{1/4}} - \frac{\mu_0^3\beta^2}{\pi(\hbar\upsilon_{\rm F})^2 B(1-\beta^2)^{1/4}}, \tag{40}$$

$$M_{\rm add}^{\rm T} = \frac{\pi\hbar\upsilon_{\rm F}\beta R_T}{BL_y}A_{M_0} - \frac{\pi\hbar\upsilon_{\rm F}\beta(2+\beta^2)}{2BL_y(1-\beta^2)}A_{\Omega_T}(R_T^*-R_T), \tag{41}$$

and

$$M_{\rm osc}^{\rm T} = -\frac{e\mu_0}{\pi\hbar}(1-\beta^2)^{3/4}\sum_{k=1}^{\infty}\frac{\sin(\pi k w)}{\pi k}R_T - \frac{(e\upsilon_{\rm F})^2 B}{2\pi\mu_0(1-\beta^2)^{1/4}}[(4-\beta^2)R_T + (2+\beta^2)(R_T^*-R_T)]\sum_{k=1}^{\infty}\frac{\cos(\pi k w)}{(\pi k)^2}, \tag{42}$$

where $R_T^*(k,\mu) = R_T^2(k,\mu)\cosh(2\pi^2 k\mu_0 k_{\rm B}T/e\hbar\upsilon_{\rm F}^2 B^*)$. Apparently, since $R_T(k,\mu)\to 1$ and $R_T^*(k,\mu)\to 1$ for $T\to 0$, equation (42) reduces to the magnetization in equation (25) for zero temperature.

As illustrated in figure 3(a), finite T causes a reduction of the magnetization amplitude as opposed to the case of $T = 0$ K. In addition, it shows the magnetization M versus reciprocal field $1/B$ for three different temperatures with a given E. It can be seen that as the value of $1/B$ increases, the OA of magnetization decreases and eventually collapses when $\beta\to 1$. Nevertheless, regarding zero temperature, there is no such a collapse for the OA of magnetization, as shown in figure 1(a). Accordingly, we attribute this to the finite temperature effect.

Figure 3(b) depicts the magnetization M as a function of E for three different temperatures with a given B. The three curves correspond to $T_1 = 20$ K, $T_2 = 30$ K and $T_3 = 100$ K, respectively. It has been shown that the magnetization decreases approximately linearly with increasing E, except in the case of $T_3 = 100$ K. Finally, the magnetization decreases to negative infinity at $\beta_{\rm c} = 1$, following equations (40)–(42). At the temperature T_3 or even a higher one, the magnetization $M\simeq 0$ rather than decreasing with increasing E. Figure 3(c) gives the magnetization M as function of the temperature T. Increasing T, the magnetization M increases for B_1, B_3, B_5 and decreases for B_2, B_4, B_6, but they all end up approaching different constants.

We get the dHvA magnetic susceptibility from the magnetization:

$$\chi_{\rm reg}^{\rm T} = \frac{3e\mu_{\rm p0}\sqrt{e\hbar}\varsigma(3/2)\upsilon_{\rm F}}{4\sqrt{2B}\pi^2\hbar(1-\beta^2)^{5/4}}(1-2\beta^2) + \frac{\mu_0^3\beta^2\mu_{\rm p0}(6-5\beta^2)}{2\pi(\hbar\upsilon_{\rm F}B)^2(1-\beta^2)^{5/4}}, \tag{43}$$

$$\chi_{\rm add}^{\rm T} = -\frac{2\mu_{\rm p0}\beta\mu_0^4 R_T}{L_y B^2(\hbar\upsilon_{\rm F})^3} + \frac{\pi\hbar\upsilon_{\rm F}\mu_{\rm p0}\beta(2+\beta^2)}{B^2 L_y(1-\beta^2)}A_{M_0}(R_T^*-R_T) - A_{\chi 0_T}A_{\Omega_T}\frac{\pi\hbar\upsilon_{\rm F}\mu_{\rm p0}\beta}{L_y}, \tag{44}$$

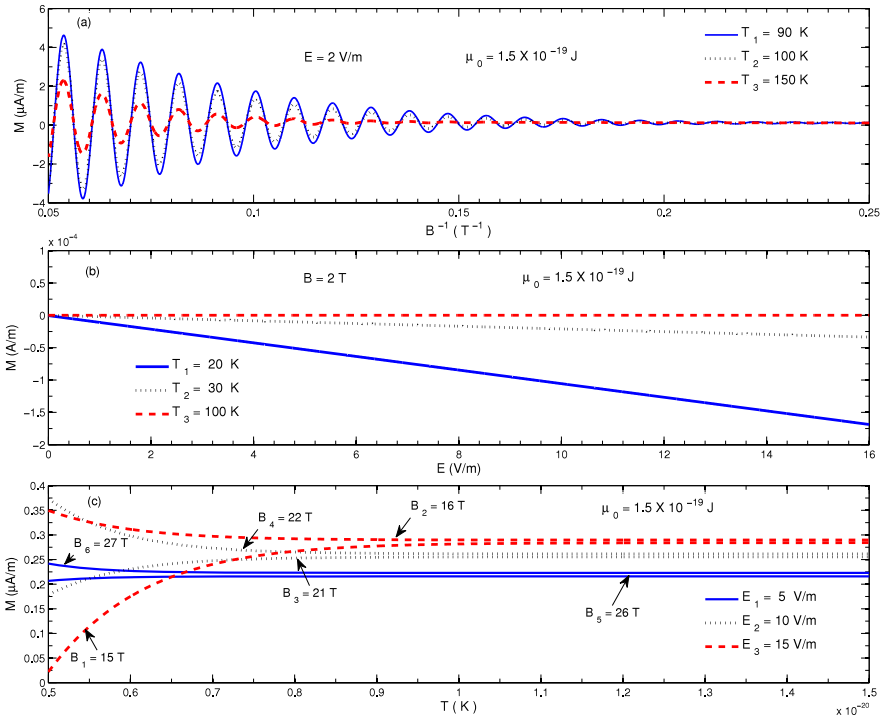

Figure 3. (a) Magnetization M is plotted as a function of reciprocal magnetic field $1/B$ for a given chemical potential $\mu_0 = 1.5 \times 10^{-19}$ J and $E = 2$ V m^{-1}. The three curves correspond to temperature $T_1 = 90$ K, $T_2 = 100$ K and $T_3 = 150$ K, respectively. (b) M plotted for electric field E with $B = 2$ T and $\mu_0 = 1.5 \times 10^{-19}$ J. The three curves correspond to $T_1 = 20$ K, $T_2 = 30$ K and $T_3 = 100$ K, respectively. (c) M is plotted as a function of temperature T for $\mu_0 = 1.5 \times 10^{-19}$ J.

and

$$\chi_{\rm osc}^{\rm T} = A_{\chi 1_T} \sum_{k=1}^{\infty} \cos(\pi k w) + A_{\chi 2_T} \sum_{k=1}^{\infty} \sin(\pi k w). \quad (45)$$

In equation (44), A_{M_0} and A_{Ω_T} are defined by equations (24) and (35), respectively. We also define

$$A_{\chi 0_T} = \frac{(2\beta^4 - 10\beta^2 - 4)}{[2B(1-\beta^2)]^2}[R_T^* - R_T] + \left(\frac{2+\beta^2}{2B(1-\beta^2)}\right)^2 \times \left[2R_T(R_T^* - R_T)\cosh\frac{2\pi^2 kT\mu_0}{e\hbar\upsilon_{\rm F}^2 B^*} - R_T^3 \sinh^2\frac{2\pi^2 kT\mu_0}{e\hbar\upsilon_{\rm F}^2 B^*} - (R_T^* - R_T)\right], \quad (46)$$

$$A_{\chi 1_T} = \frac{\mu_0^3 \mu_{\rm p0}(1-\beta^2)^{3/4}}{\pi(\hbar\upsilon_{\rm F}B)^2} R_T - \frac{(e\upsilon_{\rm F})^2 \mu_{\rm p0}(4-\beta^2)(2+\beta^2)}{2\pi\mu_0(\pi k)^2(1-\beta^2)^{5/4}} \times (R_T^* - R_T) - R_T \frac{(e\upsilon_{\rm F})^2 \mu_{\rm p0}(8-10\beta^2-\beta^4)}{4\pi\mu_0(\pi k)^2(1-\beta^2)^{5/4}} - \frac{A_{\chi 0_T}\mu_{\rm p0}(e\upsilon_{\rm F}B)^2}{\pi\mu_0(\pi k)^2}(1-\beta^2)^{3/4}, \quad (47)$$

$$A_{\chi 2_T} = -\frac{e\mu_0\mu_{\rm p0}(2+\beta^2)}{\pi^2\hbar k B(1-\beta^2)^{1/4}} R_T^*. \quad (48)$$

Figure 4(a) shows the magnetic susceptibility χ oscillates periodically as a function of $1/B$, for three characteristic temperatures, namely, 80, 100, and 150 K. Similar to the magnetization as shown in figure 3(a), it also exhibits the dependence on temperature. It can be seen clearly that finite T causes a reduction of the oscillation amplitude, and as the value of $1/B$ increases, the OA of the magnetic susceptibility finally decays to zero.

Figure 4(b) shows the magnetic susceptibility χ plotted as a function of E with a given B. The three curves correspond to $T_1 = 20$ K, $T_2 = 30$ K and $T_3 = 100$ K, respectively. For a finite temperature such as T_1 or T_2, the magnetic susceptibility decreases approximately linearly with increasing E and exhibits Landau diamagnetism in graphene supported by $\chi < 0$. In contrast, at the temperature T_3, the magnetic susceptibility $\chi \simeq 0$, stands for the disappearance of the diamagnetism in graphene. In addition, there is no increase in the magnetic susceptibility with increasing E. It warrants great attention that from equations (43)–(45), it could be inferred that the magnetic susceptibility eventually decreases to negative infinity at $\beta_{\rm c} = 1$. Figure 4(c) directly gives the magnetic susceptibility χ with respect to the temperature T. More specifically, it shows that the magnetic susceptibility χ increases with increasing T and finally approaches zero under different electric fields E and the magnetic fields B.

4. Conclusions

In summary, this paper reports on a theoretical study on the modulation of the de Haas–van Alphen effect in graphene by an electric field. Three major findings emerge from the study. First of all, we find that both magnetization and magnetic susceptibility are modulated by the electric field. At zero or finite temperature, both magnetization and magnetic susceptibility are predicted to oscillate periodically as a function of the reciprocal field $1/B$. The dHvA oscillation

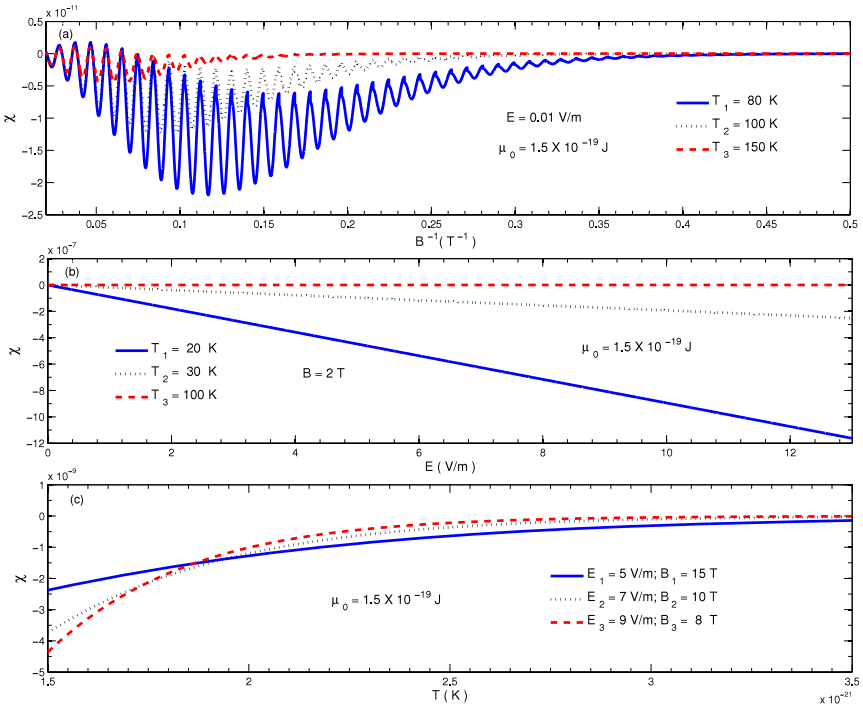

Figure 4. (a) Magnetic susceptibility χ to reciprocal field $1/B$ for a given chemical potential $\mu_0 = 1.5 \times 10^{-19}$ J and $E = 0.01$ V m^{-1}. The three oscillation curves of magnetic susceptibility correspond to $T_1 = 80$ K, $T_2 = 100$ K and $T_3 = 150$ K, respectively. (b) χ as a function of electric field E with $B = 2$ T and $\mu_0 = 1.5 \times 10^{-19}$ J. The three oscillation curves of magnetic susceptibility correspond to $T_1 = 20$ K, $T_2 = 30$ K and $T_3 = 100$ K, respectively. (c) χ as a function of temperature T for $\mu_0 = 1.5 \times 10^{-19}$ J.

period $\Delta(1/B)$ is derived analytically. It is also discovered that as the parameter β increases, the values of magnetization and magnetic susceptibility finally increase to positive infinity or decrease to negative infinity at the exotic point $\beta_c = 1$. Furthermore, the analytical results indicate that the dHvA oscillation amplitude increases abruptly to infinity for zero temperature at $\beta_c = 1$, but eventually collapses at a finite temperature, directly leading to the vanishing of the de Haas–van Alphen effect. The 'vanishing' is accounted for by the anomalous effect of the electric field on the Landau level, which arises from the instability of the relativistic quantum field vacuum. In addition, it is established that the magnetic susceptibility depends on the electric and magnetic fields, which suggests that graphene should be a non-linear magnetic medium. These phenomena, not available in the standard 2D electron gas, are deemed as the consequence of the relativistic type spectrum of low energy electrons and holes in graphene.

Acknowledgments

We thank Dr D Q Liu, Q Wang, X H Zhang, B H Gong, L Xu, and H W Chen for helpful discussions. This work is supported by the Cultivation Fund of the Key Scientific and Technical Innovation Project, Ministry of Education of China (No. 708082).

References

[1] Novoselov K S, Geim A K, Morozov S V, Jiang D, Zhang Y, Dubonos S V, Grigorieva I V and Firsov A A 2004 *Science* **306** 666
[2] Novoselov K S, Jiang D, Schedin F, Booth T J, Khotkevich V V, Morozov S V and Geim A K 2005 *Proc. Natl Acad. Sci. USA* **102** 10451
[3] Zhang Y, Small J P, Amori M E S and Kim P 2005 *Phys. Rev. Lett.* **94** 176803
[4] Li G and Andrei E Y 2007 *Nat. Phys.* **3** 623
[5] Kane C L and Mele E J 2005 *Phys. Rev. Lett.* **95** 226801
[6] Haldane F D M 1988 *Phys. Rev. Lett.* **61** 2015
[7] Sinitsyn N A, Hill J E, Min H, Sinova J and MacDonald A H 2006 *Phys. Rev. Lett.* **97** 106804
[8] Yao W, Yang S A and Niu Q 2009 *Phys. Rev. Lett.* **102** 096801
[9] Wilson M 2006 *Phys. Today* **59** 21
[10] Novoselov K S, Geim A K, Morozov S V, Jiang D, Katsnelson M I, Grigorieva I V, Dubonos S V and Firsov A A 2005 *Nature* **438** 197
[11] Zhang Y B, Tan Y W, Stormer H L and Kim P 2005 *Nature* **438** 201
Zhang Y, Jiang Z, Small J P, Purewal M S, Tan Y W, Fazlollahi M, Chudow J D, Jaszczak J A, Stormer H L and Kim P 2006 *Phys. Rev. Lett.* **96** 136806
[12] Sharapov S G, Gusynin V P and Beck H 2004 *Phys. Rev.* B **69** 075104
[13] Peierls R 1933 *Z. Phys.* **81** 186
[14] Landau L D and Lifshitz E M 1971 *Relativistic Quantum Theory* (New York: Pergamon) p 100
[15] Lukose V, Shankar R and Baskaran G 2007 *Phys. Rev. Lett.* **98** 116802
[16] Callaway J 1976 *Quantum Theory of the Solid State* (New York: Academic)
[17] Shoenberg D 1984 *Magnetic Oscillations in Metals* (Cambridge: Cambridge University Press)
[18] Gradshtein I S and Ryzhik I M 1980 *Table of Integrals, Series and Products* (Orlando, FL: Academic)
[19] Wilde M A, Schwarz M P, Heyn C, Heitmann D, Grundler D, Reuter D and Wieck A D 2006 *Phys. Rev.* B **73** 125325
[20] Simserides C 2009 *J. Phys.: Condens. Matter* **21** 015304
[21] Hu J and MacDonald A H 1992 *Phys. Rev.* B **46** 12554